



The natural ocean acidification and fertilization event caused by the submarine eruption of El Hierro

SUBJECT AREAS:
VOLCANOLOGY
BIOGEOCHEMISTRY
GEOCHEMISTRY
MARINE CHEMISTRY

J. M. Santana-Casiano¹, M. González-Dávila¹, E. Fraile-Nuez², D. de Armas², A. G. González¹, J. F. Domínguez-Yanes² & J. Escánez²

¹Departamento de Química. Universidad de Las Palmas de Gran Canaria. 35017 Las Palmas de Gran Canaria. Spain, ²Instituto Español de Oceanografía. Centro Oceanográfico de Canarias. 38180 Santa Cruz de Tenerife. Spain.

Received
2 October 2012

Accepted
11 January 2013

Published
25 January 2013

Correspondence and requests for materials should be addressed to J.M.S.-C. (jmsantana@dqui.ulpgc.es)

The shallow submarine eruption which took place in October 10th 2011, 1.8 km south of the island of El Hierro (Canary Islands) allowed the study of the abrupt changes in the physical-chemical properties of seawater caused by volcanic discharges. In order to monitor the evolution of these changes, seven oceanographic surveys were carried out over six months (November 2011–April 2012) from the beginning of the eruptive stage to the post-eruptive phase. Here, we present dramatic changes in the water column chemistry including large decreases in pH, striking effects on the carbonate system, decreases in the oxygen concentrations and enrichment of Fe(II) and nutrients. Our findings highlight that the same volcano which was responsible for the creation of a highly corrosive environment, affecting marine biota, has also provided the nutrients required for the rapid recuperation of the marine ecosystem.

Submarine volcanoes inject large amounts of material of variable size, texture and chemical composition into the oceans¹. The state of the eruptive evolution of the volcano ranges from ongoing magmatic activity to a highly evolved hydrothermal system. Lava flows, bubbles of lava, lava debris, ash, pumice, steam-blast eruptions, hydrothermal vents, plumes of fine materials and dissolved gas, explosions and discoloration of sea water to light-blue and reddish brown have been observed in several eruptions^{1,2}.

While subaerial volcanoes are well characterised, there is a lack of study of those in the submarine setting^{3–6}. Direct observations of submarine eruptions have been scarce, as they are hard to predict and they occur in remote locations⁷. Monitoring these volcanoes is an objective which is not easy to achieve. The first registered underwater eruption was that of the NW Rota 1 in the southwest Pacific Ocean at the Marina Arc⁸ in 2006 with a summit depth of 517 m and in 2011, the second, the West Mata volcano in the Lau Basin⁹, that was monitored at 1200 m. Recently, the dynamic cycle of growth in the Monowai underwater volcano has been described¹⁰. However, most of the knowledge about the chemistry of underwater volcanism comes from the studies related to hydrothermal vents at great depths. Observations of submarine eruptions have been more common in the Pacific^{7–12} compared to the Atlantic Ocean^{13–16}. In all cases the carbonate system is modified, and the pH reduced as a consequence of the emission of magmatic gas and other compounds¹⁷. Moreover, the emission of reduced species contributes to the reduction of the redox potential and the decrease in the amount of dissolved oxygen in the system.

The island of El Hierro is the western island of the Canary Archipelago located in the north-eastern Atlantic Ocean (Fig. 1a). It is the youngest island with 1.12 Million years of age¹⁸. In July 2011, the seismic stations deployed by the National Geographical Institute (IGN) in El Hierro recorded the start of unusual seismic activity, indicating the beginning of volcanic unrest. More than 12,000 earthquakes were registered prior to the onset of volcanic tremor on October 10th 2011, suggesting the beginning of a submarine eruption¹⁹. Seven hydrographic cruises (Table S1, Supplementary Information) allowed the study of the evolution of changes in the physical-chemical parameters in the ocean. The pH in total scale at 25°C (pH_T), total dissolved inorganic carbon (C_T), and total alkalinity (A_T), were measured together with temperature, salinity, dissolved oxygen and total sulfur reduced species. Nutrients, ferrous iron, and pCO₂ were also analysed on most of the cruises. As a result of the ongoing magmatic activity, the submarine eruption produced an unprecedented episode of severe acidification and fertilization. These phenomena were studied throughout the duration of the eruptive process from the beginning of the eruptive stage, where the affected area covered the entire area southwest and northwest of the island, to the post-eruptive phase where the affected area was reduced to 0.5 km around the volcano.

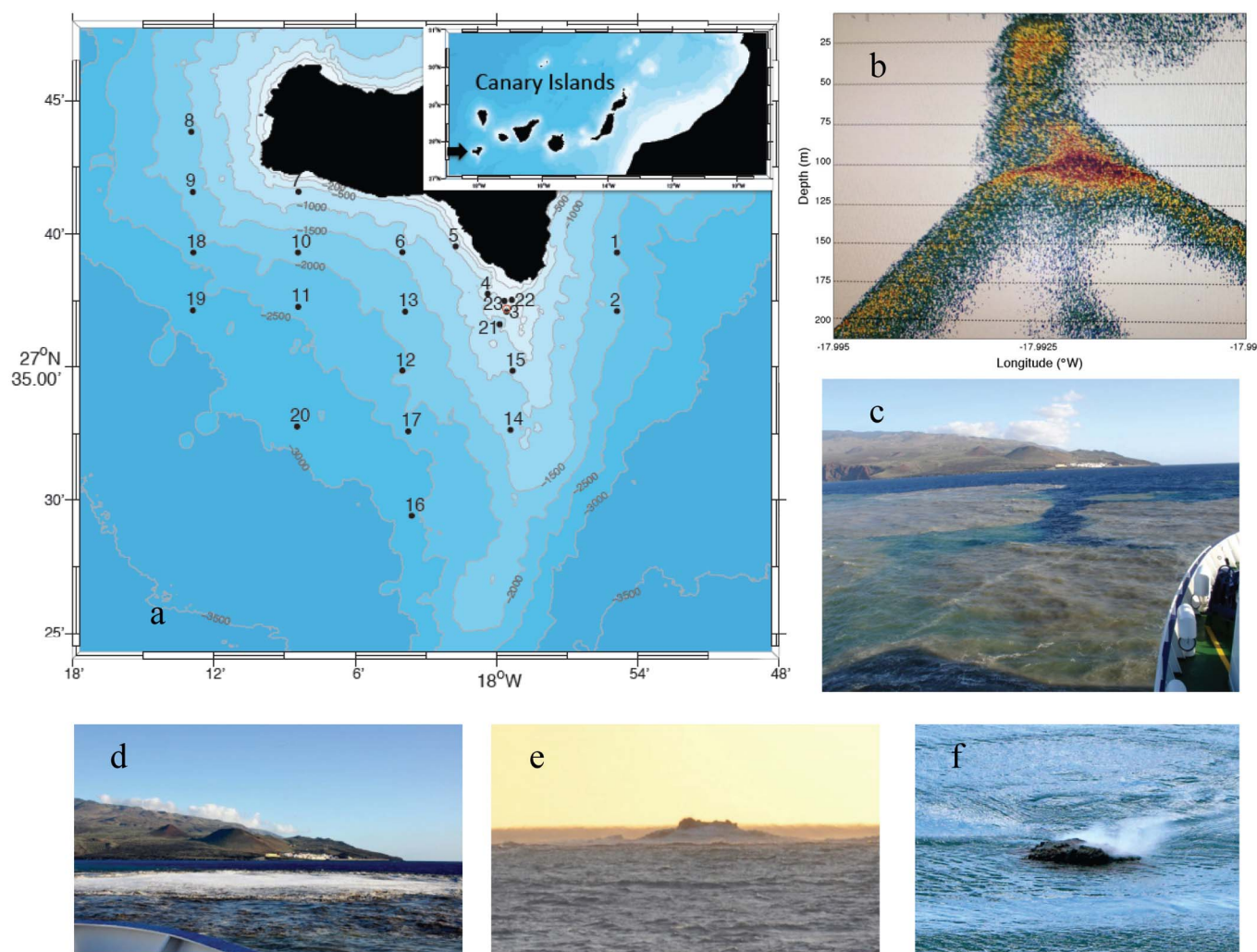


Figure 1 | The El Hierro 2011 eruption. (a) Localization of the stations carried out during Leg 3 in the island of El Hierro. (b) Echogram of the volcanic cone from a 70 kHz echo sounder in April 2012. (c) Colour patches in the surface water in the area related to the discharge of high temperature hydrothermal fluids as well as magmatic gases and volcanic particles. (d) The surface seawater bubbling due to the submarine eruption, on November 5th 2011. (e) A 10-meter high bubble emerged during the afternoon on November 5th 2011. (f) Floating rocks degassing on the ocean surface.

Results

The submarine eruption of the island of El Hierro was the first one to be monitored from the initial unrest and also the first submarine eruption reported in about 600 years of historical records in the Canary Islands. The eruption started in October 11th 2011, evidence of the eruption was observed in the sea surface. A discoloration of the surface water in the area was observed, ranging from light-green, to milky-blue to a dark brown colour. These changes were related to the discharge of high temperature hydrothermal fluids as well as magmatic gases and volcanic particles^{1,20}. Bubbling and degassing took place, and abundant rock fragments were found floating on the ocean surface during the first months of the eruption (Fig. 1b–f). The strongest episodes of bubbling took place between November 5th and 8th with large bubbles which reached 10–15 m in height (Fig. 1e).

On October 23th, the R/V *Ramón Margalef* (IEO) undertook the first survey in the volcanically affected area and the base of the active volcano was found at a depth of 350 m at 27°37'07"N – 017°59'28"W. The volcano was located on a rift with the lava flowing south-westwards. The volcano was 650 m wide and its peak was situated at a depth of 220 m below sea level. In January 2012, the cone had risen to a depth of 130 m and in February it reached its maximum elevation of 88 m below sea level^{21,22} (Fig. 1b). While both the structure and the height of the volcanic edifice were changing, the emission plume was also being modified. Additionally, in the surface,

the plume was affected by the changing meteorological conditions in the area.

The acidification of the area and the changes in the carbonate system. The lack of steady state conditions during the eruption produced highly variable chemical properties in the water column. The strongest eruptive episode occurred during Leg 3 on November 5th 2011 (Fig. 1e) when observations of highly elevated total dissolved inorganic carbon coupled with large decreases in alkalinity and pH_T were made (Table 1). At that time, when the cone was more than 200 m below sea level, the lowest values of pH_T were concentrated in a layer of 75–100 m depth at most of the stations, but due to the intensity of the ejected gases, low values of pH_T also reached the surface waters.

Figure 2a depicts the distribution of pH_T values at *in situ* conditions at four selected depths during the first week of November 2011, where station 1 represents a typical vertical distribution for pH_T in the Canary basin²³. The pH values throughout the text are expressed as pH_T *in situ* conditions. During Leg 3, surface seawater chemistry around the entire southwest end of the island was highly altered, with pH_T values as low as 5.1 in close proximity to the volcano increasing to 6.5 in the surrounding area. In the layer at 75–100 m depth, the effects of the emissions were more localised around the volcano with pH_T values of between 5.8 and 6.4 which increased to values between



Table 1 | Extreme values for the carbonate system measured at station 3 for the different cruises (depth in m; temperature T in °C, Salinity S, pH in total scale at *in situ* conditions, $p\text{CO}_2$ in μatm , $\text{pH}_{\text{T, is}}$, C_{T} , A_{T} and $[\text{O}_2]$ in $\mu\text{mol kg}^{-1}$). For comparative purposes, values measured at surface waters in station 1 (reference), unaffected by the volcano, were also included

Date	Cruise	Depth	T	S	$\text{pH}_{\text{T, is}}$	C_{T}	A_{T}	$p\text{CO}_2$	O_2
5-Nov-11	Leg 3	5	23.913	36.858	5.134	7,681.5	1,338.0	230,316	112.9
17-Nov-11	Leg 5	79	20.920	36.196	5.201	12,015.0	1,153.0	316,832	0
8-Dec-11	Raprocan	7	21.633	36.771	5.403	9,515.1	2,139.9	220,753	175.5
14-Jan-12	Leg 8	7	20.510	36.963	5.655	5,414.1	2,165.5	107,610	185.8
10-Feb-12	Leg 10	6	19.770	36.859	6.121	3,403.5	2,211.8	38,891	161.6
25-Feb-12	Leg 12	7	18.793	36.780	6.251	3,583.0	2,482.3	33,148	164.1
7-Apr-12	Cetobaph	7	19.523	36.964	7.322	2,469.0	2,457.0	2,660	232.0
8-Apr-12	Cetobaph	126	18.555	36.748	6.115	4,190.6	2,685.6	47,161	214.8
5-Nov-11	Reference	5	23.549	37.065	8.045	2,113.7	2,430.1	414	217.2

7.2 and 7.6 to the southwest of the volcano (St. 11, 12, 17 and 20). At 400 m depth, a patch of seawater with pH_{T} values between 7.2 and 7.4 was located to the southwest of the volcano (St. 12 and 17) while at stations 13, 15 and 19, the observed pH_{T} value was 7.80, 0.2 units below the pH_{T} in the unaffected areas (7.98).

The C_{T} in the surface waters around the volcano was as high as 7,682 $\mu\text{mol kg}^{-1}$ (Fig. 2b). To the west, and following the direction of the volcanic plume, the C_{T} values decreased gradually to 2,780 $\mu\text{mol kg}^{-1}$ (Sts. 6, 11, 13 and 20). Normal surface C_{T} values of 2,100 $\mu\text{mol kg}^{-1}$ were detected in stations 1 and 18. At a depth of 75 m, at station 21, the closest point to the South of the volcano, the C_{T} was 4,526 $\mu\text{mol kg}^{-1}$. An area of 100 km^2 to the southwest of the volcano presented average values of 2,700 $\mu\text{mol kg}^{-1}$. As was similarly observed for the pH_{T} , at 400 m depth, the C_{T} was also affected, with values ranging between 2,350 and 2,400 $\mu\text{mol kg}^{-1}$.

During Leg 5 from November 16th to 20th, the volcanically affected area was visited twice. During the first visit, surface pH_{T} values for stations 4 and 5 were 5.70 and 6.28, respectively, while surface waters at station 3 remained unaffected ($\text{pH}_{\text{T}} = 8.05$) due to the prevailing northwest currents. However, station 3 exhibited extraordinarily large changes in carbonate chemistry at 80 m depth with pH_{T} and alkalinity as low as 5.20 and 1153 $\mu\text{mol kg}^{-1}$ respectively, with C_{T} as high as 12,015 $\mu\text{mol kg}^{-1}$ and $p\text{CO}_2$ calculated from pH_{T} and C_{T} to be as high as 316,832 μatm . Similar results were observed for stations 4 and 5 at the same depth. During the second visit, the same conditions were observed at station 3 while at station 4 the effect was only observed in the layer between 75–125 m depth (at 125 m, $\text{pH}_{\text{T}} = 6.04$, $C_{\text{T}} = 4,057$ $\mu\text{mol kg}^{-1}$, $A_{\text{T}} = 2213$ $\mu\text{mol kg}^{-1}$, $p\text{CO}_2(\text{pH}, C_{\text{T}}) = 49,888$ μatm). This was a consequence of a change in the direction of the surface currents.

In December 2011 (Raprocan1211 cruise) the carbonate chemistry at station 3 in the surface waters was the most anomalous: 5.40 for the pH_{T} , C_{T} of 9,515 $\mu\text{mol kg}^{-1}$, A_{T} of 2140 $\mu\text{mol kg}^{-1}$ and $p\text{CO}_2(\text{pH}, C_{\text{T}})$ of 232,490 μatm . In the upper 300 m of the water column around the volcano, pH_{T} was < 7, except in the layer at 125–150 m depth where the pH was 7.90. Similar effects from the emission of magmatic CO_2 were observed in January 2012 during Leg 8.

In April 2012, the eruption had stopped and the system evolved to a hydrothermal system. The pH_{T} in the whole water column outside of the volcanically affected area was the typical for the Canary basin, with anomalous pH_{T} values found only in an area within a radius of 500 m around the cone. Directly above the cone, the pH_{T} measured at the surface waters was 7.3, while at 50 m depth, the value was 7.2. The seawater in proximity to the crater had pH_{T} values of just 6.1, while the C_{T} increased to 4,191 $\mu\text{mol kg}^{-1}$. However, unlike the observations of decreases in alkalinity during most of the eruptive phase, the alkalinity increased above the natural values of around 2400 $\mu\text{mol kg}^{-1}$ to 2686 $\mu\text{mol kg}^{-1}$ (Table 1 and Table S4, Supplementary Information). Increased A_{T} values were also observed at the end of February close to the volcanic cone, when the activity

decreased, and can be related to changes in the compounds and reactions that influence the carbonate system throughout the eruptive process.

Fluxes of CO_2 to the atmosphere during the explosive episode.

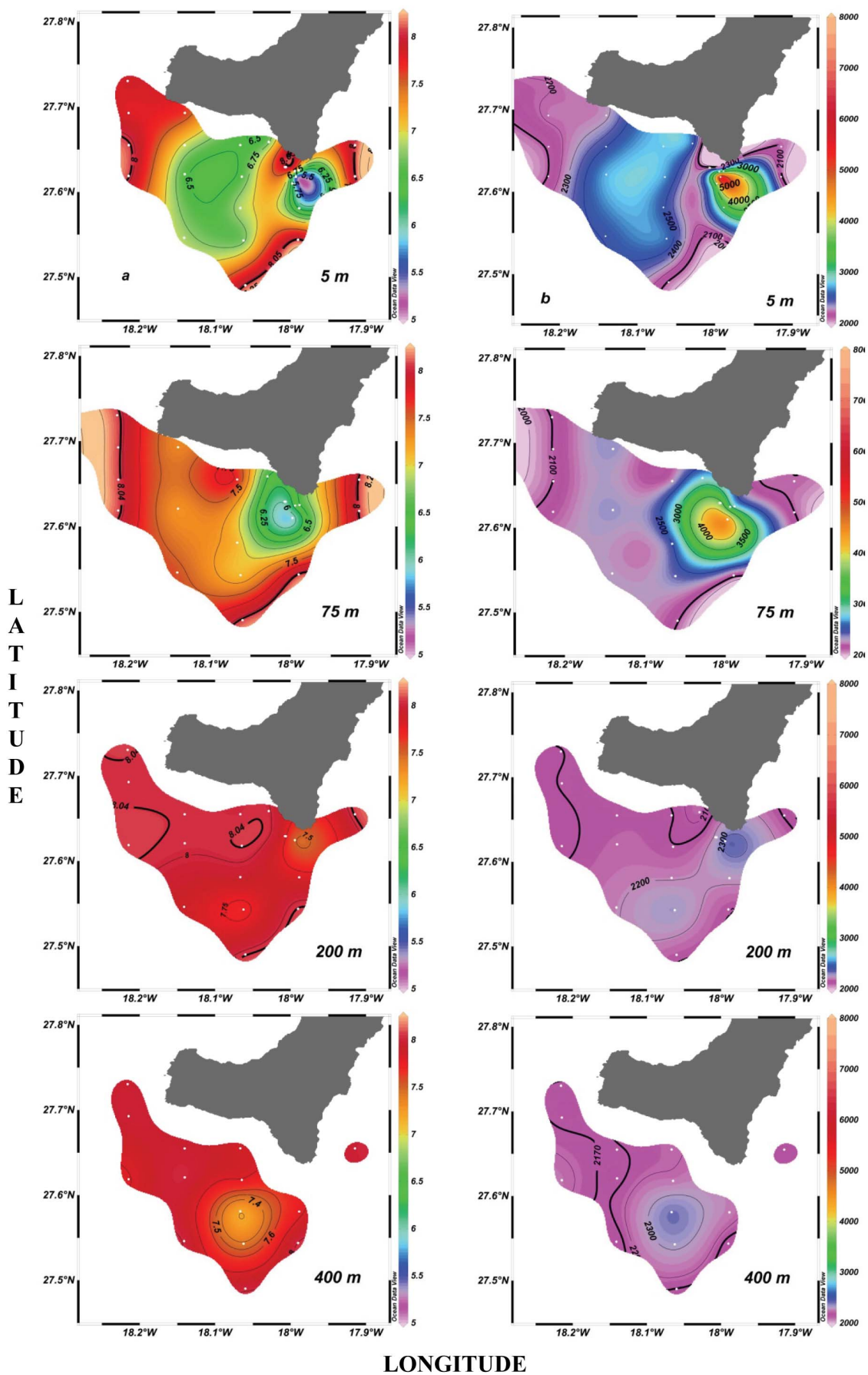
During Leg 3 (Fig. 3), the CO_2 emitted by the volcano increased the $p\text{CO}_2(\text{pH}, C_{\text{T}})$ to values as high as 155,000 μatm in station 3, reaching 223,400 μatm just after a 10 meter high bubble emerged in November 5th (Fig. 1e). The surface seawater to the southwest of the island had $p\text{CO}_2(\text{pH}, C_{\text{T}})$ values in the range of 11,000 to 19,000 μatm . Measured $p\text{CO}_2$ in the areas unaffected by the volcanic emissions were of 414 ± 2 μatm , in accordance to computed $p\text{CO}_2(\text{pH}, C_{\text{T}})$. During the week of the explosive event (November 4th to 9th), a flux of CO_2 of 5×10^{10} g d^{-1} was computed²⁴ for the 385 km^2 area covered by this Leg (shaded area in Fig. 3) by using a weekly mean wind speed of 7.5 m s^{-1} . This amount of CO_2 is equivalent to 0.08% of the global CO_2 flux²⁵.

Emissions of reduced S species, Fe(II), nutrients and changes in the Oxygen concentration. During the period of volcanic activity, the emission of reduced sulfur species (H_2S , HS^- , S^{2-} , S^0 , SO_3^{2-} , S_x^{2-} , $\text{S}_2\text{O}_3^{2-}$, $\text{S}_4\text{O}_6^{2-}$) and Fe(II) (Fe^{2+} , $\text{Fe}(\text{OH})^+$, $\text{Fe}(\text{OH})_2$, FeCl^+ , $\text{Fe}(\text{HCO}_3)^+$, FeHS) contributed to decreases in both the redox potential and the concentration of dissolved oxygen in the system (Fig. 4).

Reduced sulfur species were measured from Leg 5 onwards. Detectable dissolved reduced sulfur was determined in the stations close to the volcano with maximum values of 476 $\mu\text{mol kg}^{-1}$ at 75 m depth (at station 3) on November 17th 2011 (Fig. 4). Surface waters for the volcanically affected area had sulfur values between 50 and 132 $\mu\text{mol kg}^{-1}$, with the maximum value observed at station 3 in December. The concentration of dissolved sulfur at 75–100 m depth decreased progressively during the time of the study. By February 2012 (Leg 10, data not shown), sulfur was only detected in surface waters above the volcano (40 $\mu\text{mol kg}^{-1}$) while in April 2012 reduced sulfur species values were below the detection limit.

The volcanic emissions also introduced a large amount of Fe(II) into the water column (Fig. 4), which was strongly correlated with the pattern observed for the sulfur reduced species. In November 17th, the concentration of total Fe(II) reached maximum values of 50 $\mu\text{mol kg}^{-1}$ at 75 m depth at station 3. On December 8th a maximum value of 20 $\mu\text{mol kg}^{-1}$ was measured in the surface waters. Normal dissolved Fe(II) values²⁶ in the surface ocean are < 0.2 nM which is five orders of magnitude below the values determined for total Fe(II) in the volcanic area.

A size speciation study was carried out on December 8th at station 23 (Fig. 5a). Total Fe(II) concentration in surface waters was 12.7 $\mu\text{mol kg}^{-1}$, with a secondary maximum of 4 $\mu\text{mol kg}^{-1}$ at 100 m depth. At the bottom, the total Fe(II) concentration increased again reaching a value of 4 $\mu\text{mol kg}^{-1}$. In surface waters 64% of the total Fe(II) was particulate (8.1 $\mu\text{mol kg}^{-1}$), while dissolved



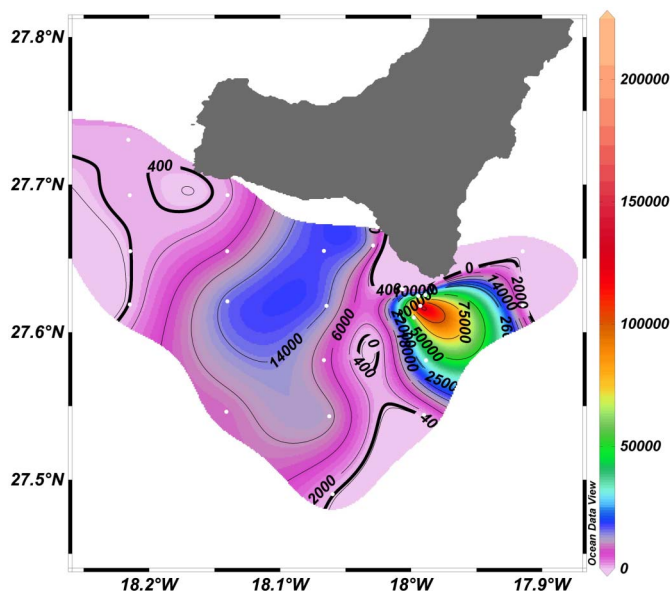


Figure 3 | Surface distribution of the partial pressure of CO₂. Surface $p\text{CO}_2(\text{pH,CT})$ (μatm) distribution in the southwest of the island of El Hierro during Leg 3.

Fe(II) ($< 0.1 \mu\text{m}$) accounted for 26% of the total, ($3.3 \mu\text{mol kg}^{-1}$). Over 95% of the total Fe(II) at 100 m was present as particulate Fe ($> 0.45 \mu\text{m}$), while dissolved Fe(II) was 2.8% (110 nmol kg^{-1}).

The presence of these reduced species produced low redox potentials (Fig. 4) which reached values of -0.03 V at 100 m depth in station 3 and values of 0.15 V in surface waters at station 4, where the maximum values of Fe(II) and reduced sulfur species were found, on November 20th. Low redox potential with values below 0.05 V were only recorded at the station above the volcano during January and February 2012. Background redox potential is 0.2 V and was observed at station 1.

The flux and oxidation of Fe(II) and reduced sulfur species^{27–29} were so high that oxygen values were often below detection limit. Patches of anoxia at 100 m depth in the volcanically affected area were determined at station 3 on November 5th (data not shown) and at stations 4 and 5 on November 16th (Fig. 4, Table 1). Minimum values of around $100 \mu\text{mol kg}^{-1}$ of oxygen were also observed during other visits to those stations in November 2011. The low oxygen concentrations in these waters together with the low pH_T values contributed to the high mortality of marine biota which was observed in the area after the first two months of the eruption.

During the eruption the same pattern observed for C_T and reduced species was also found in the vertical profiles for nutrients in all of the cruises (Fig. 5). In November, the maximum values were obtained around 100 m depths while in December, they were found in surface waters. Nitrate concentrations as high as $3 \mu\text{mol kg}^{-1}$ were found in the surface waters, while at 100 m depth values increased to $8 \mu\text{mol kg}^{-1}$. Phosphate values increased one order of magnitude in the layer of 100–125 m depth, reaching maximum values of $0.6 \mu\text{mol kg}^{-1}$. Silicate concentration in surface waters showed values as high as $17 \mu\text{mol kg}^{-1}$ in December and $15 \mu\text{mol kg}^{-1}$ in February. In November, a value of $23 \mu\text{mol kg}^{-1}$ was measured at 100 m depth.

Discussion

In the oceanic regions where submarine volcanoes experience magmatic or hydrothermal activity, the water properties change^{3,17}. The reactions which mainly explain the variations in pH_T values^{27,30} are shown in Table 2. The changes observed in pH_T are a consequence of the emissions of CO₂, SO₂ and H₂S/HS⁻ from the submarine volcano (reactions 1–5, Table 2). As soon as the volcanic fluid mixes with

seawater, the dissolved reduced species, Fe(II), Mn(II) and H₂S/HS⁻, are oxidised, consuming oxygen and acidifying the system (reactions 5 and 6–8). The emission of Fe(II) also contributed to acidifying the system due to the reaction of Fe(II) with H₂S (reaction 9). Part of this decrease is compensated by reactions (10–12) that also contribute to increase the alkalinity. The CO₂-weathering reaction (12) has been described in gas-rich hydrothermal systems³¹ after H⁺ reacts with the host rock.

The pH_T of the seawater column in the volcanically affected area during the explosive episode changed drastically, reaching values < 6 , with the largest anomaly, $\Delta\text{pH} = 2.9$, detected close to the volcano (Table 1). This decrease in pH represents 81,370% increase in the proton concentration. Six months later, during the April cruise, after the eruption had stopped, the composition of the gases close to the summit was primarily CO₂ with a complete absence of dissolved reduced species, which caused a decrease of pH_T values to 6.1, 1.9 units below the normal values.

An attempt was made to quantify the effect of each contributor to the carbonate system change in the area affected by the volcano (Supplementary Information). The model indicated that the emitted CO₂ (Table 2, reactions 1 and 2) contributed to up to 95% of the observed decrease in pH during the first 3 months. The remaining unexplained contribution is related to the role of reactions (3) to (12). From the end of February onwards, when the eruptive activity had concluded, anomalous values of alkalinity were determined, with $A_{T,\text{exp}} > A_{T,\text{ref}}$ and $\text{pH}_{\text{exp}} > \text{pH}_{A_{T,\text{ref}},\text{CT}}$, that indicated a major role was played by mineral alkalinity species³ and reactions 9 to 12 (Table 2 and Supplementary information).

The potential of volcanic emissions to fertilize the ocean has been subject to speculation over the years¹. The volcanic activity releases nutrients into the seawater³², including Fe, Si, P and N. The deposition of volcanic ash onto the surface ocean has been found to increase Fe concentrations³³ to 0.4 to 2.4 nmol L^{-1} . During the submarine eruption of the island of El Hierro, values of total Fe(II) were as high as $50 \mu\text{mol kg}^{-1}$ at 75 m depth. In surface waters (Fig. 4a), from a value of total Fe(II) of $12.7 \mu\text{mol kg}^{-1}$, $3.3 \mu\text{mol kg}^{-1}$ were dissolved and thus bio-available for the marine organisms³⁴. The low pH_T conditions would contribute both to favour the presence of higher amounts of iron in its reduced state, due to a decrease in Fe(II) oxidation rates²⁹, and to an increase in the Fe(III) solubility³⁵, and consequently, augment the amount of bio-available iron for the biological community. However, the Canary Islands are found in an oligotrophic area^{23,36}. Nutrient concentrations to the south of the island of El Hierro are undetectable in the first 80–100 m of depth. During the volcanic eruption an important input of nutrients was observed. The increased amount of nutrients in the euphotic zone, together with the high dissolved iron concentrations, may contribute to the regeneration of productivity in the area. The results emerging from this study show how the same volcano responsible for eradicating most of the marine life in the waters south of the island of El Hierro also provides the ingredients bringing the affected area back to life.

Methods

Cruises. Two weeks after the start of the eruption, an oceanographic research program was initiated by the Instituto Español de Oceanografía (IEO) to localise the exact position of the submarine eruption, to perform a periodic bathymetric surveys of the area, and to study the evolution of the physical-chemical anomalies in the ocean produced by magmatic activity. Over six months, an unprecedented oceanographic investigation was carried out. The name given to this study was *Bimbache*, the name of the original inhabitants of the island of El Hierro. The study was divided into 12 legs where geophysical and physical-chemical oceanographic researches were alternatively organised (Table S1, Supplementary Information). In addition, two more hydrographical cruises were carried out in the area (Raprocan and Cetobaph).

Hydrography. Vertical profiles of conductivity, temperature, pressure and oxygen were collected using a SeaBird 9/11-plus CTD equipped with dual conductivity and temperature sensors. CTD sensors were calibrated at the SeaBird laboratory before the cruise. Water samples were obtained using a rosette of 24-10-liter Niskin bottles.

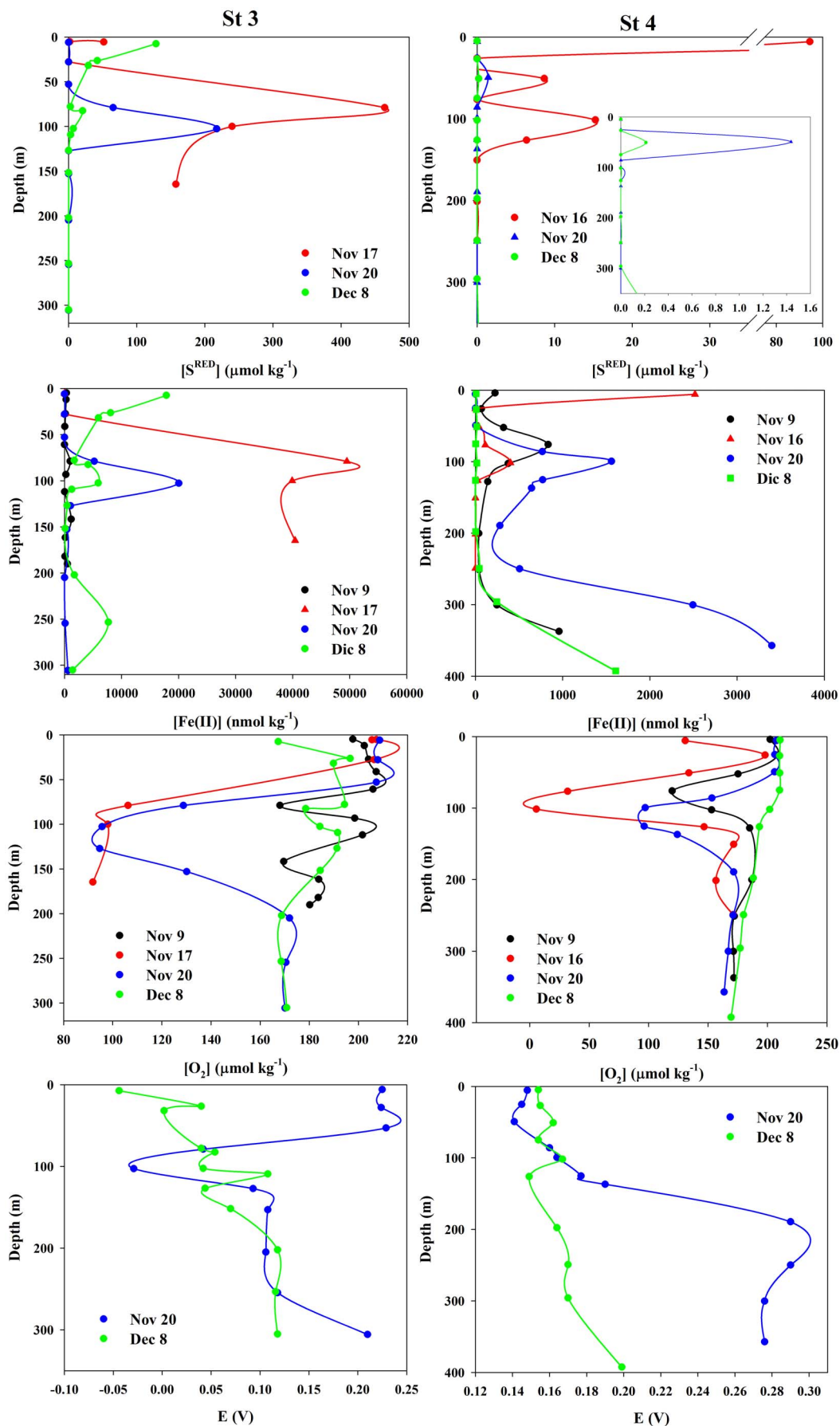


Figure 4 | Evolution of the concentration of reduced species close to the volcano. Vertical profiles of reduced sulfur species (S^{RED}), total Fe(II) and oxygen concentrations ($\mu\text{mol kg}^{-1}$), and Redox Potential (E, Volts), at stations 3 and 4 in November and December 2011.

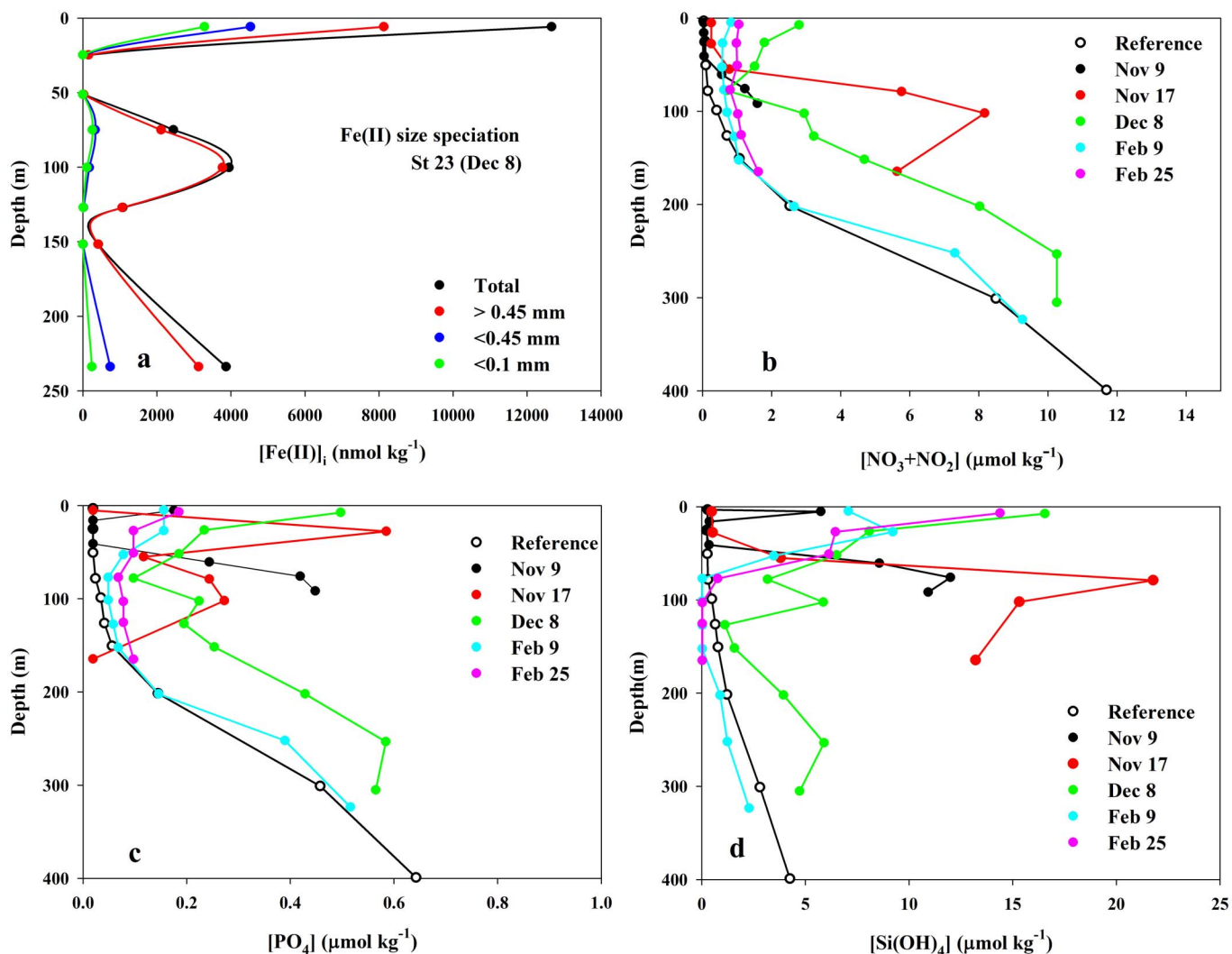


Figure 5 | Fe(II) speciation and nutrients. (a) Fe(II) speciation for station 23 close to the volcano on December 8th, 2011. Fe(II) fractionation is indicated in the methods section. Evolution of the concentrations of (b) nitrate + nitrite ($\text{NO}_2^- + \text{NO}_3^-$, $\mu\text{mol kg}^{-1}$), (c) phosphate (HPO_4^{2-} , $\mu\text{mol kg}^{-1}$) and (d) silicate (Si(OH)_4 , $\mu\text{mol kg}^{-1}$) at station 3. The profile for a reference station is also included.

Acoustics. Vessel-mounted Simrad EK60 (38 and 70 kHz) split-beam echosounders were used to collect acoustic data.

pH. The pH in the total scale at a constant temperature of 25°C ($\text{pH}_{\text{T},25}$) was measured spectrophotometrically³⁷ with m-cresol purple as an indicator²⁴ (the dye effect was removed for each pH reading) with an uncertainty of 0.002 units. In the stations which were strongly affected by the volcanic emissions, the $\text{pH}_{\text{T},25}$ was also measured by potentiometry with an OrionTM combine glass electrode calibrated with TRIS buffer solutions³⁸.

A_T, C_T and pCO₂. A VINDTA 3C system (Marianda company) was used for both total alkalinity and total dissolved inorganic carbon concentration determination. The titration of certified reference material for oceanic CO₂, CRMs (#105), was used to test the performance of the equipment. Measurements of CRMs were within $\pm 1.0 \mu\text{mol kg}^{-1}$ of the certified value for both parameters. The computation of other carbonate variables (pCO_2) and values at in situ conditions ($\text{pH}_{\text{T},is}$) was done by using the CO2sys.xls v12 programme³⁹ and the set of constants of Mehrbach *et al.*⁴⁰ as in Dickson and Millero⁴¹. During the Leg 3 the partial pressure of CO₂, pCO_2 , was computed using the pair pH_{T} , C_T. In all other cruises, pCO_2 was also computed and

Table 2 | Reactions affecting the pH and alkalinity of the seawater due to the volcanic emissions

Reaction	Number
$\text{CO}_2 + \text{H}_2\text{O} = \text{H}_2\text{CO}_3$	1
$\text{H}_2\text{CO}_3 = \text{H}^+ + \text{HCO}_3^-$	2
$3 \text{SO}_2 + 2 \text{H}_2\text{O} = \text{S(0)} + 2 \text{H}_2\text{SO}_4$	3
$4 \text{SO}_2 + 4 \text{H}_2\text{O} = \text{H}_2\text{S} + 3 \text{H}_2\text{SO}_4$	4
$\text{H}_2\text{S} + 2 \text{O}_2 = \text{H}_2\text{SO}_4$	5
$\text{Mn(II)} + \frac{1}{2} \text{O}_2 + \text{H}_2\text{O} = \text{MnO}_2 + 2 \text{H}^+$	6
$\text{Fe(II)} + \frac{1}{4} \text{O}_2 + \text{H}_2\text{O} = \frac{1}{2} \text{Fe}_2\text{O}_3 + 2 \text{H}^+$	7
$\text{FeS} + \frac{9}{8} \text{O}_2 + \text{H}_2\text{O} = \frac{1}{2} \text{Fe}_2\text{O}_3 + \text{H}_2\text{SO}_4$	8
$\text{Fe(II)} + \text{H}_2\text{S} = \text{FeS} + 2 \text{H}^+$	9
$\text{FeS} + 4 \text{MnO}_2 + 8 \text{H}^+ = 4 \text{Mn(II)} + \text{SO}_4^{2-} + \text{Fe(II)} + 4 \text{H}_2\text{O}$	10
$\text{FeS} + 2 \text{Fe(OH)}_3 + 6 \text{H}^+ = 3 \text{Fe(II)} + \text{S(0)}$	11
$2 \text{NaAlSi}_3\text{O}_8 + 2 \text{CO}_2 + 3 \text{H}_2\text{O} = \text{Al}_2\text{Si}_2\text{O}_5(\text{OH})_4 + 2 \text{Na}^+ + 2 \text{HCO}_3^- + 4 \text{SiO}_2$	12



measured by using a continuous PRO-Oceanus $p\text{CO}_2$ system. Due to sensor calibration limitations, the values of $p\text{CO}_2$ over 1000 μatm were determined from C_T and pH. The nutrient data, determined as indicated in González-Dávila *et al.*²³ was also considered in the computation. Oxygen concentrations were measured on board by Winkler titration.

Reduced Sulfur (S) species. Total reduced S (H_2S , HS^- , S^{2-} , S^0 , SO_3^{2-} , $\text{S}_2\text{O}_3^{2-}$, $\text{S}_4\text{O}_6^{2-}$) was determined ($\pm 1 \mu\text{mol Kg}_{\text{sw}}^{-1}$) by the iodometric method^{42,43} using an automated potentiometric titration monitored by a platinum electrode. Prior to the start of the titration the same platinum electrode was used to measure the redox potential, E(V).

Fe(II). The concentration of Fe(II) was determined by the modified version of the Ferrozine method^{29,44}. The detection limit of the method was 1nM of Fe(II). Seawater samples (15 ml) were fixed with 100 μl of trace metals grade pure HCl (Aldrich) for the determination of total Fe(II). Total Fe(II) was defined as the ferrous iron dissolved in the sample at pH 1. For the analysis, samples were diluted with iron-free seawater at pH 1 when necessary in order to achieve a concentration in the nanomolar range. For the size speciation study, prior to acidification, seawater was filtered by 0.45 μm and 0.1 μm filters and collected in a container with 100 μl of HCl. The particulate Fe was defined as the difference between the measured total dissolved Fe(II) in the pure acidified sample and the Fe(II) obtained from samples filtered by 0.45 μm filters. Dissolved Fe(II) was measured in samples that had been filtered by 0.1 μm .

- Mantas, V. M., Pereira, A. J. S. C. & Morais, P. V. Plumes of discolored water of volcanic origin and possible implications for algal communities. The case of the Home Reef eruption of 2006 (Tonga, Southwest Pacific Ocean). *Rem. Sen. Environ.* **115**, 1341–1352 (2011).
- Siebert, L. & Simkin, T. Volcanoes of the world: An illustrated catalogue of Holocene volcanoes and their eruptions, Smithsonian Institution, Global Volcanism Program Digital Information Series, GVP-3 (2001).
- Resing, J. A. *et al.* Chemistry of hydrothermal plumes above submarine volcanoes of the Mariana Arc. *Geochem. Geophys. Geosyst.* **10**, Q02009 (2009).
- de Ronde, C. E. J. *et al.* Submarine hydrothermal activity along the mid-Kermadec Arc, New Zealand: large-scale effects on venting. *Geochem. Geophys. Geosyst.* **8**, Q07007 (2007).
- Embley, R. W. *et al.* Explorations of Mariana arc volcanoes reveal new hydrothermal systems. *EOS Trans. AGU* **85**, 37–40 (2004).
- Resing, J. A. *et al.* Venting of acid-sulfate fluids in a high-sulfidation selting at NW Rota 1 submarine volcano on the Mariana Arc. *Econ. Geol.* **102**, 1047–1061 (2007).
- Mitchell, C. Hot, cracking rocks deep down. *Nature Geosci.* **5**, 444–445 (2012).
- Embley, R. W. *et al.* Extensive and diverse submarine volcanism and hydrothermal activity in the NE Lau Basin. *Eos Trans. AGU* (Fall Meeting Supplement) **90**, abstr. V51D–1719 (2009).
- Resing, J. A. *et al.* Active submarine eruption of boninite in the northeastern Lau Basin. *Nature Geosci.* **4**, 799–806 (2011).
- Watts, A. B. *et al.* Rapid rates of growth and collapse of Monowai submarine volcano in the Kermadec Arc. *Nature Geosci.* **5**, 510–515 (2012).
- Cheminée, J.-L. *et al.* Gas-rich submarine exhalations during the 1989 eruption of Macdonald Seamount. *Earth Planet. Sci. Lett.* **107**, 318–327 (1991).
- Duennebie, F. K. *et al.* Researchers rapidly respond to submarine activity at Loihi Volcano, Hawaii. *EOS Trans. Am. Geophys. Un.* **78** (22), 229, 232–233 (1997).
- Carey, S. & Sigurdsson, H. Exploring submarine arc volcanoes. *Oceanogr.* **20**, 80–89 (2007).
- Malmberg, S. A. A report on the temperature effect of the Surtsey eruption on the sea water. *Surtsey Res. Prog. Rep. I*, pp. 6–9, Surtsey Res. Soc., Reykjavik, Iceland (1965).
- Malmberg, S. A. Beam transmittance measurements carried out in the waters around Surtsey, 1–2 August, 1966. *Surtsey Res. Prog. Rep. IV*, pp. 193–202, Surtsey Res. Soc., Reykjavik, Iceland (1968).
- Forjaz, V. H. *et al.* Notícias sobre o Vulcão Oceânico da Serreta, Ilha Terceira dos Açores. Ed. Observatório Vulcanológico e Geotérmino dos Açores (eds.), Ponta Delgada, 40 p (2000).
- Resing, J. A. & Sansone, F. J. The chemistry of lava-seawater interactions: the generation of acidity. *Geochim. Cosmochim. Acta* **63**, 2183–2198 (1999).
- Guillou, H. *et al.* K-Ar ages and magnetic stratigraphy of a hotspot-induced, fast grown oceanic island: El Hierro, Canary Islands. *J. Volcanol. Geotherm. Res.* **73**, 141–155 (1996).
- López, C. *et al.* Monitoring the volcanic unrest of El Hierro (Canary Islands) before the onset of the 2011–2012 submarine eruption. *Geophys. Res. Lett.* **39**, L13303 (2012).
- Nogami, K., Yoshida, M. & Osaka, J. Chemical composition of discolored seawater around Satsuma-Iwojima, Kagoshima, Japan. *Bull. Volcanol. Soc. Japan* **38**, 71–77 (1993).
- Acosta, J. & Rivera, J. Informes de campaña BIMBACHE1011-11. Instituto Español de Oceanografía (2012).
- Fraille-Nuez, E. *et al.* The submarine volcano eruption of El Hierro Island: physical-chemical perturbation and biological response. *Sci. Rep.* **2**, 486 (2012).
- González-Dávila, M. *et al.* The influence of island generated eddies on the carbon dioxide system south of the Canary Islands. *Mar. Chem.* **99**, 177–190 (2006).
- González-Dávila, M. *et al.* Seasonal and interannual variability of sea surface carbon dioxide species at the European Station for Time Series in the Ocean at the

- Canary Islands (ESTOC) between 1996 and 2000. *Global Biogeochem. Cycles* **17**, 1076 (2003).
- Peters, G. P. *et al.* Rapid growth in CO_2 emissions after the 2008–2009 global financial crisis. *Nature Climate Change*, **2**, 2–4 (2011).
- Gerringa, L. J. A. *et al.* Co-variance of dissolved Fe-binding ligands with phytoplankton characteristics in the Canary Basin. *Mar. Chem.* **102**, 276–290 (2006).
- Rickard, D. & Luther III, G. W. Chemistry of iron sulfides. *Chem. Rev.* **107**, 514–562 (2007).
- Zhang, J. Z. & Millero, F. J. The products from the oxidation of H_2S in seawater. *Geochim. Cosmochim. Acta* **57**, 1705–1718 (1993).
- Santana-Casiano, J. M., González-Dávila, M. & Millero, F. J. Oxidation of nanomolar level of Fe(II) with oxygen in natural waters. *Environ. Sci. Technol.* **39**, 2073–2079 (2005).
- Soetaert, K. *et al.* The effect of biogeochemical processes on pH. *Mar. Chem.* **105**, 30–51 (2007).
- Sedwick, P. N. *et al.* Chemistry of hydrothermal solutions from Pele's Vents, Loihi Seamount, Hawaii. *Geochim. Cosmochim. Acta* **56**, 3643–3667 (1992).
- Olgun, N. *et al.* Airborne volcanic ash trace metal release to the surface ocean and possible effects on marine primary production. *Geophys. Res. Abstracts*, **10**, EGU2008-A-06029 (2008).
- Duggen, S. *et al.* Subduction zone volcanic ash can fertilize the surface ocean and stimulate phytoplankton growth: Evidence from biogeochemical experiments and satellite data. *Geophys. Res. Lett.* **34**, L01612 (2007).
- Shaked, Y., Kustka, A. B. & Morel, F. M. M. A general kinetic model for iron acquisition by eukaryotic phytoplankton. *Limnol. Oceanogr.* **50**, 872–882 (2005).
- Liu, X. & Millero, F. J. The solubility of iron in seawater. *Mar. Chem.* **77**, 43–54 (2002).
- Pelegri, J. L. *et al.* Coupling between the open ocean and the coastal upwelling region off northwest Africa: water recirculation and offshore pumping of organic matter. *J. Mar. Syst.* **54**, 3–37 (2005).
- Clayton, T. D. & Byrne, R. H. Spectrophotometric seawater pH measurements: total hydrogen ion concentration scale calibration of m-cresol purple and at-sea results. *Deep Sea Res. I* **40**, 2115–2129 (1993).
- Millero, F. J. The pH of estuarine seawater. *Limnol. Oceanogr.* **31**, 839–847 (1986).
- Lewis, E. D. & Wallace, W. R. *Program developed for CO_2 system calculations*. Report 105, Oak Ridge National Laboratory, US Department of Energy, Oak Ridge, Tennessee (1998).
- Mehrbach, C. *et al.* Measurement of the apparent dissociation constants of carbonic acid in seawater at atmospheric pressure. *Limnol. Oceanogr.* **18**, 897–907 (1973).
- Dickson, A. G. & Millero, F. J. A comparison of the equilibrium constants for the dissociation of carbonic acid in seawater media. *Deep-Sea Res.* **34**, 1733–1743 (1987).
- Konovalov, S. K. *et al.* Intercalibration of CoMSBlack-93a chemical data; unification methods for dissolved oxygen and hydrogen sulfide analyses and sampling strategies of CoMSBlack-94a cruise. *Rep. Inst. Mar. Sci. Edermil, Turkey* (1994).
- Konovalov, S. K. & Romanov, A. S. Spectrophotometric and iodometric methods for the detection of hydrogen sulfide in the Black Sea: comparison of the results of analysis. *Phys. Oceanogr.* **10**, 365–377 (1999).
- González-Dávila, M., Santana-Casiano, J. M. & Millero, F. J. Oxidation of iron(II) nanomolar with H_2O_2 in seawater. *Geochim. Cosmochim. Acta* **69**, 83–93 (2005).

Acknowledgements

This work was supported by the Instituto Español de Oceanografía, IEO, by the European Project CARBOCHANGE contract 264879 and by the Spanish Government, Ministerio de Economía y Competitividad, through the ECOFEMA CTM2010-19517 Project. The CETOBAPH-CGL2009-1311218 Project provided us the opportunity to visit the volcano in April 2012. We thank the Captains of the R/V Ramón Margalef and R/V Cornide Saavedra, and their crews for their help during this research. J.A. Resing is thanked for the comments in his review which improved the report.

Author contributions

The paper was written by JMS-C and MG-D. Data analysis and interpretation was carried out by JMS-C, MG-D, EF-N. Observational data was provided by JMS-C, MG-D, EF-N, DdA, AG, FD and JE. All the authors discussed the results and contributed to the manuscript.

Additional information

Supplementary information accompanies this paper at <http://www.nature.com/scientificreports>

Competing financial interests: The authors declare no competing financial interests.

License: This work is licensed under a Creative Commons Attribution-NonCommercial-NoDerivs 3.0 Unported License. To view a copy of this license, visit <http://creativecommons.org/licenses/by-nc-nd/3.0/>

How to cite this article: Santana-Casiano, J.M. *et al.* The natural ocean acidification and fertilization event caused by the submarine eruption of El Hierro. *Sci. Rep.* **3**, 1140; DOI:10.1038/srep01140 (2013).